

Cellular Material Fatigue Estimation And Development

Eren Pehlivan¹

¹CTU in Prague, Faculty of Mechanical Engineering, Department of Mechanics, Biomechanics and Mechatronics, Technická 4, 166 07 Prague 6, Czech Republic

Abstract

To develop porous metal that mimic the architecture and mechanical properties of the natural bone is a new approach in bio-medical application. The microstructure and cellular architecture of these metallic foams dictates their mechanical behavior. This study attempts to improve the fundamental understanding of the fatigue behavior of titanium foam as well as control the life time of the porous structure according changing mesh architecture.

Keywords:

Porosity, Titanium Foams, Cellular Structure

1. INTRODUCTION

Porosity structure is also known as a cellular solid and it consists of interconnected network such as edges and faces of cells. One of the well known example hexagonal cells of bee and that is the reason it calls honeycombs. The honeycombs foundation idea of porosity structure in two dimension geometry. Therefore, it helps to understand simplified porosity structure [1].

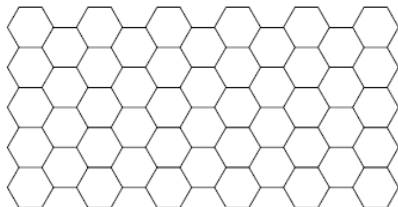


Figure 1. Regular Honeycombs.

It is considered, three dimensions cellular structure would be defined as a foam shape which consist of interconnected networks like honeycombs such as edges and faces of the cells. However, Shape is more likely resemble convex hull.

Two typical types of cellular structures, lightweight structures and compliant mechanisms, have been investigated up to now. Lightweight structures are rigid and designed to reduce weight, while increasing strength and stiffness. Compliant mechanisms are designed to transform motions and forces. However, the performance of lightweight structures can be enhanced by using adaptive cellular structures with conformal strut orientations and sizes, like the trabecular shape in femoral bone.

Trabecular bone exists at the ends of the long bones, within the vertebral body, and in the core of shell-like bones such as the skull. It has a cellular structure, with a relative density typically between about 0.05 and

0.3. Bone grows in response to load, so that the density of trabecular bone depends on the magnitude of the loads and the orientation of the trabeculae depends on the direction of the loading. Low-density trabecular bone resembles an open-cell foam. High-density trabecular bone has a more plate-like structure [2].

There are several ways to produce foam titanium as well as additive manufacturing is getting reaching more people every day. The term rapid prototyping (RP) is used in a variety of industries to describe a process for rapidly creating a system or part representation before final release or commercialization. In other words, the emphasis is on creating something quickly and that the output is a prototype or basis model from which further models and eventually the final product will be derived [3].

In order to produce cellular titanium product in variety geometry, selective laser sintering (SLS) and electron beam melting (EBM) are widely used particularly in medical device and aerospace industry. All additive manufacturing (AM) applications consists of the same idea and approach which can be described as layer by layer building as well as range of materials. Laser additive manufacturing (LAM) is considered as an one of them and has ability to provide high-performance metallic components with controllable micro structural and mechanical properties.

Selective Laser Sintering consist on integration of a powder layers using a laser beam (for instance: Nd-YAG or CO₂) and it is designed for manufacturing models of tools and prototypes. The selection of adequate parameters allows to melt or sinter a metal powder particles in precisely definite areas. A whole process (processing or mirco-processing) is controlled by program [4].

Electron Beam Melting (EBM) is a rapid manufacturing process in which fully solid parts with properties equal to those of shaped materials are built on a

layer by-layer basis. After melting and solidifying one layer of titanium powder, the process is repeated for following layers until the part is complete.

In medical market recently have a number of porosity structure implants. 3D printed lumbar cage spinal implant is one of them and they have produced by Stryker and Zimmer which are the well known medical companies. It is a huge advantage to modify different section stiffness of the implant in order to reduce stress shielding effect. Moreover, vast of the bone contain trabecular cells shape with different size. For instance, another well know 3D printed orthopedic implant is acetabular cup which manufactured by Smith & Nephew. Although both implant contain the same structure even the same manufacturing technique, with different cell size. Cell size is one of the important subject when bone and implant interaction is considered.

The multiphase interconnected morphology of bone tissue and other natural structures have inspired the development of more advanced composite materials. These include the ones in which the matrix phase cannot be distinguished from the reinforcement phase as in conventional composites. In conventional composites, a discrete reinforcement phase is embedded in a matrix phase. As a consequence, the elements of the reinforcement phase are isolated from one another, and only the matrix phase can be considered three dimensionally connected. In contrast, interpenetrating phase composites (IPC) are multiphase composites in which all individual phases are intermingled and co-continuous in a 3D space [5]. As it was mentioned above that bone and cellular structure together create a IPC composition.

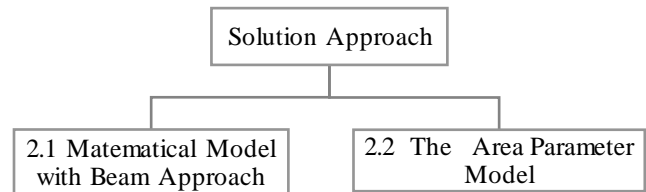
The A4 paper format should be used for writing the full text. The page margins should be set to 2 cm except the top margin which is 2.5 cm. Use a two-column format with the space between the columns set to 8 mm. The title, authors, affiliations, abstract, and keywords are typed in one-column format.

The header margin is set to 1.2 cm, the footer to 1.4 cm. Headers in all pages (except the first one) should contain the following text "Student's conference 2016 | Czech Technical University in Prague | Faculty of Mechanical Engineering" centred. In the footer of the first page, the text "Corresponding author: " followed by an email address of the first author should be inserted (everything set in Times, 9 pt, left aligned with a line of thickness 0.25 mm and length 5 cm placed 1 mm above the text). Do not add any page numbers.

1. METHOD AND TECHNIQUE

In order to tackle porosity structure fatigue problem, several approaches were considered. One of the main thing to be considered is, solution will be in Meso or Macro level. In this section Meso-level solution was carried out with mathematical model which consist of beams according to Timoshenko beam theory. The macro level solution approach is ideally related to test result.

Area parameter model approach was developed by Murakami and in this paper will try add further features to equation in order to cover the test results.



2.1. Mathematical Model With Beam Approach

Mechanical performance of the porosity structure is affected by several dynamics such as

- Properties of solid it is made from ($\rho_s, E_s, \sigma_{ys}...$)
- Relative density, ρ^* / ρ_s
- Cell geometry
- Cell shape
- Foams - open vs. closed cells

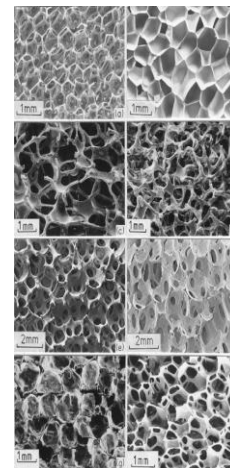


Figure 2. Porosity Structure types

Unit cell approach one of the technique gives a chance to compare analytic calculation and finite element method. This technique evaluate the computer base calculation because when cells number increase FEM will be the approach must used. As it was mentioned that mathematical models of foam simplified as a honeycombs. Therefore, unit cell is choose as a hexagonal geometry which can be seen in figure 3.

Young modulus for a unit hexagonal cell was calculated with displacement and momentum in order to gain delivered an analytical phrase. For a regular hexagonal honeycomb (Figure 3.) with linear elastic walls of uniform thickness, t , side length, l , and Young's modulus, E

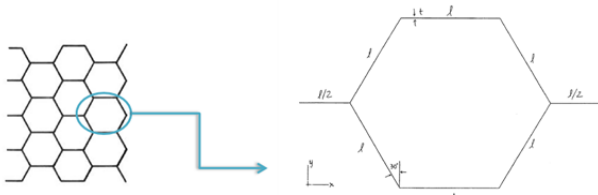


Figure 2. Unit honeycomb cell.

Theoretical calculation of young modulus in the plane;

$$\frac{E_x}{E_s} = \frac{E_y}{E_s} = \frac{4}{\sqrt{3}} \left(\frac{t}{l}\right)^3$$

E_x^* and E_y^* are Young's modulus in the x- and y- directions, respectively. The thickness to length ratio, t/l is given as a function of the relative density $\frac{\rho^*}{\rho_s}$ by

$$\left(\frac{t}{l}\right) = \frac{\sqrt{3}}{2} \left(\frac{\rho^*}{\rho_s}\right)$$

This equation is used by condition under $t/l < 0.2$. equation about can be only use small t/l values. It was also calculated an analytical expression for the yield strength of a hexagonal unit cell with elastic-perfectly plastic cell walls [6].

$$\left(\frac{t}{l}\right) < 3 \left(\frac{\sigma_{ys}}{E_s}\right)$$

Otherwise, plastic collapse occurs when the bending moment in the cell walls reaches the fully plastic moment. When the two moments are balanced, the plastic yield stress of the regular hexagon reduces to;

$$\frac{\sigma_x}{\sigma_s} = \frac{\sigma_y}{\sigma_s} = \frac{2}{3} \left(\frac{t}{l}\right)^2$$

In order to reach analytic calculation results, wall thickness, relative density, wall length young modulus are defined;

$$\left. \begin{array}{l} \text{Wall thickness (t)} \\ \text{Wall length (l)} \end{array} \right\} t/l = 0.13$$

Relative density, consider as 0.15

Young modulus (E) $E=1$

$$E_x/E_s = E_y/E_s = 4/\sqrt{3} (t/l)^3$$

$$\sigma_x/\sigma_s = \sigma_y/\sigma_s = 2/3 (t/l)^2$$

are used in order to find Young modulus components, x and y directions.

Unit hexagonal honeycomb finite element calculation is carried out Abaqus software. Each network wall define

as a beam (According to Timoshenko Beam Theory). Therefore, Beam were decided as B22 mesh element. Abaqus input file (Inp.) was prepared by "Autocad" software and design as a regular hexagon and exported to dxf. file format for "gCAD3D" software that would help to transform dxf. file to Inp. file.



Table 1. Unit honeycomb cell

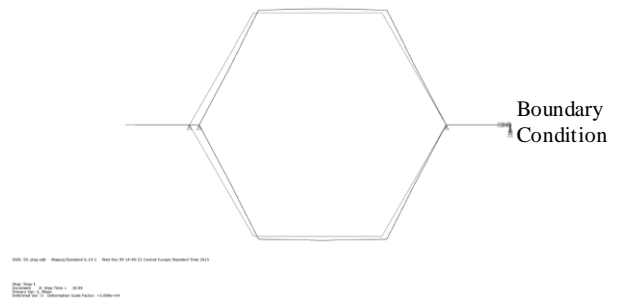


Figure 3. Unit honeycomb cell deflection results in Abaqus

X and Y direction of Young modulus and yield strength result calculated. In order to reach x direction of Young modulus force was applied in x direction which can be seen in fig4. and boundary condition was applied end of the regular hexagonal honeycomb.

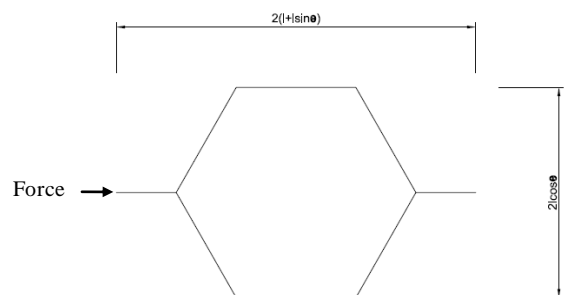


Figure 4. Regular hexagonal honeycombs general dimensions

$$\sigma_x = \frac{F_x}{2bl\cos\theta}$$

$$\epsilon_x = \frac{U_x}{2(l + l\sin\theta)}$$

Stress, strain and x direction of Young modulus components were calculated by using reaction force and displacement. First equation gives us a stress contribution of x direction and second equation explain strain in x direction. Afterwards x direction of Young modulus can be calculated by using following equation.

$$E_x = \frac{\sigma_x}{\epsilon_x}$$

Analytic results and finite element results were compared and %6.5 difference was found. Result satisfied to move further complex calculation. Developed FEM approach of unit hexagonal cell can be use d for complex and not regular structure 2D and 3D.

Printed material is considered as a perfect condition however, some of the network component might not weld or laser beam may miss the powder. Following calculation shows that concept of regularity and network reduction results. Developing new approach in order to understand simple 2D porosity structure may help to move complex 3D models in order to reduce computational cost.

First of general regular honeycombs defined with according $t/l=0.13$, $E=1$ and $\gamma=0.3$ condition. Moreover, all structures have 5 hexagonal cells of rows and 11 hexagonal cells of columns. Figure.5 illustrates general features.

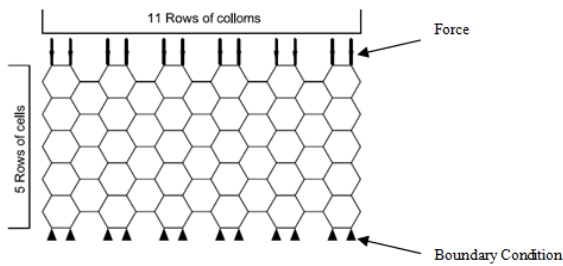


Figure 5. Regular hexagonal honeycombs

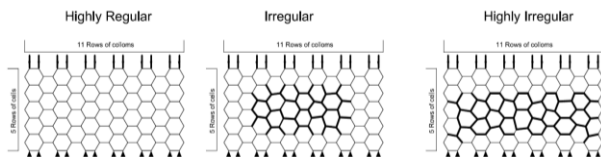


Figure 6. Hexagonal honeycombs

Figure 6 shows that 3 types of structure investigated in order to understand different mesh architecture results. Bold network lines represents modifications. Therefore, highest Von Mises stress distribution location can be changed and adjusted. It would create a huge difference during implant design and avoiding stress shielding. Moreover, high stress would effect fatigue performance as well, and implant failure can be postponed which increase patient life quality.

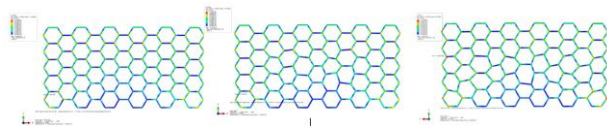


Figure 7. Hexagonal honeycombs Abaqus Von Mises stress distribution.

B22 beam structure were used for FEM calculation. Fig.8 shows that maximum Von misses stress location effected by honeycombs architecture. Maximum stress location gives an idea to redesign structure and avoiding high stress on the corners.

Maximum stress on the bar or connector of the beam would help to develop fatigue estimation as well so, it can be applied fatigue bar or rounded beam approach. Initial crack approach were used in order to identify failure beam for applying semi crack technique.

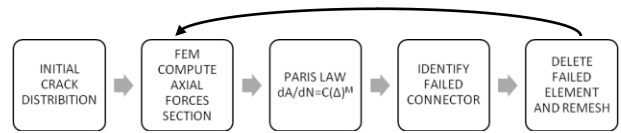


Table 2. Beam Approach Fatigue Work Flow

Semi-elliptical surface crack was used in order to discover trabecular bone behaviour. Therefore, understanding of failure connector could apply to common porosity structure fatigue problem [7]. The failure beam can be picked according to highest stress distribution. In addition, the highest bending moment occurred in the same beam with highest stress point. There is a valid ratio between diameter of the beam and initial crack and it is $a_0=d/4$ respectively.

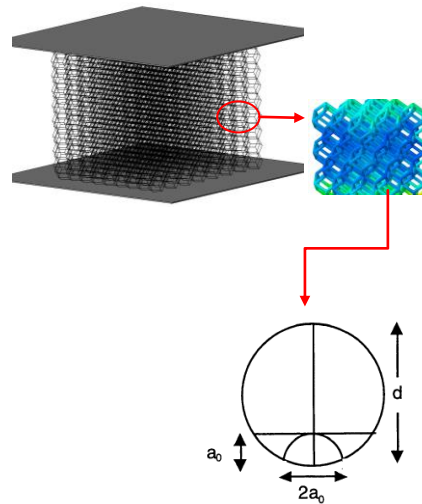


Figure 8. Geometry of semi-circular surface crack on beam cross-section. The initial crack length a_0 at the crack front was set to 1/4 of the trabecular diameter, d

"G" is known as a the strain energy release rate and three modes of the stress intensity factors are used together for three modes of loading according to Anderson,1995 work. Moreover, components of the "K" represent opening, sliding and tearing modes. " μ " is a shear modulus and second equation represent it [8].

$$G = \frac{K_I^2}{E} + \frac{K_{II}^2}{E} + \frac{K_{III}^2}{\mu}$$

$$\mu = \frac{E}{2(1+\nu)}$$

$$G = \frac{K_I^2}{E}$$

$$K_{I\text{eff}} = \sqrt{GE}$$

$$K_{I\text{eff}} = \sqrt{K_I^2 + K_{II}^2 + K_{III}^2(1+\nu)}$$

Combination of total effects of the three loading modes.

Previous work of semi-elliptical surface crack geometries contains stress intensity factors study for surface crack in a three-dimensional cylindrical beam [9].

The worst case scenario was assumed that micro-crack occurred in the condition was mentioned before. Levan and Royer have defined that stress intensity factor function is related to dimension of the beam [10].

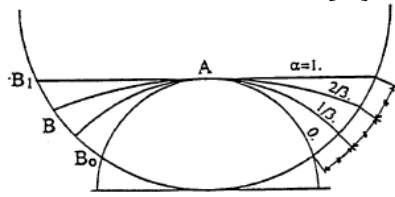


Figure 9. Crack shapes for the surface cracks defined by parameter a . (from Levan and Royer, 1993)

$$\left. \begin{aligned} \sigma_b &= \frac{4\sqrt{SM_1^2 + SM_2^2}}{\Pi r^3} \\ \sigma_\tau &= \frac{SF_1}{\Pi r^2} \\ \tau_m &= \frac{2SM_3}{\Pi r^3} \end{aligned} \right\} K_{Ieff} \propto \sigma \sqrt{\Pi a}$$

Based on previous studies, geometric parameter of the beam contains relationship with stress intensity factor. Well known equation consist of bending and tension stress analysis factor. Of course in the geometry we created or exist structure does not have sliding mode. Bending moment σ_b , axial stress σ_t and twisting moment τ_m were calculated for each beam using result were received from FEA calculation.

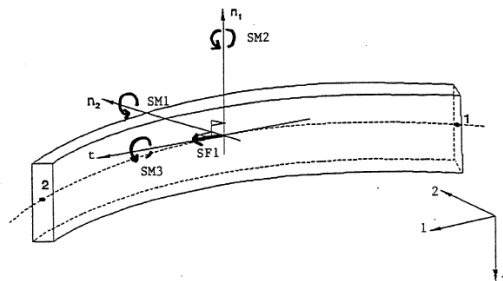


Figure 10. Geometry of beam and stress values. Finite element modelling software was used to compute the axial force $SF1$, bending moments $SM1$ and $SM2$, and twisting moment $SM3$ with respect to the local coordinate system of each beam element. After an element failed, the element

The micro-crack were supposed to be growing under cyclic loading by the Paris law [13]. Number of cycles to failure has to be recorded. The failed beam is deleted from the model, and the new mesh is generated for new analyzed using the FEA. Number of iteration is supposed to be created in order to analyse failed beams and find out life time of the structure. For further studies representative model would be created according to FEA results in order to apply for different geometry life time expectation.

2.2. The area parameter model

Previous studies shows that design lifetime of many components often exceeds 107 loading cycles, which means that components can reach to very high cycle fatigue (VHCF). In this fatigue regime, non-metallic inclusions are known to have a much detrimental effect on the fatigue performance of high-strength steels [12]. Non-metallic inclusion is one of the case for metal structure that contains pores. That would be the main reason that it may be used in additive manufacture structure (AM) due to the fact that 3D printed material consists of pores (Porosity Structure). Researchers have established the Area1/2 parameter model by which we can predict the fatigue strength of components whose fracture origin is a small defect or non-metallic inclusion [13].

Murakami demonstrated that if the fatigue fracture origin is non-metallic inclusion, the fatigue limit is determined by the matrix Vickers hardness, HV, and the square root of the projected area of the defects, area1/2. Next, they proposed the fatigue limit prediction equations (the area1/2 parameter model) taking the residual stress into consideration. They showed that the fatigue limit of high strength steels can be predicted accurately by this area1/2 parameter model [14][15].

\sqrt{area}	square root of the inclusion projected area perpendicular to the applied stress axis	m_A	material constant for Paris law crack propagation rate
Hv	Vickers hardness	$\frac{da}{dN}$	
K_{th}	threshold value of internal small crack	σ_a	applied stress
$K_{I(max)}$	applied stress intensity factor	σ_a^H	fatigue strength for high cycle fatigue
ΔK	stress intensity range	σ_w^H	fatigue strength for very high cycle fatigue
N_f	number of cycles to failure	b	Basquin exponent
b	Basquin exponent	C_A	material constant for Paris law
C_A	material constant for Paris law	σ_f'	fatigue strength coefficient

Figure 10. Content of Area Approach components

Almost % 90 of fatigue life in the "Very High Cycle Fatigue" occurs according to optical dark area (ODA) or granular-bright facet (GBF). Paris law is still suitable for small crack in VHCF [16]. Moreover, initial stress intensity factor contains relationship with total fatigue life in order to calculate fatigue life time by using integration of power law. Previous study shows that VHCF regime S-N curve may be covered by area approach.

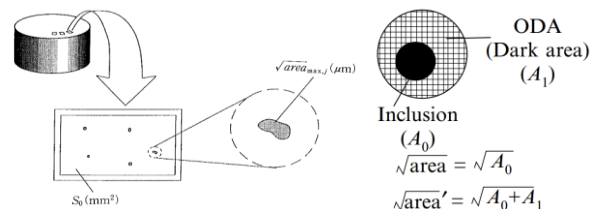


Figure 11. Optical dark are

In addition, previous studies for solid structures which has small unwanted pores effect the life time, especially larger optical dark are provide longer life time. Stretching S-N curves in our calculation some of the dynamics such as optical dark are, granular bright facet and non-metallic inclusions are supposed to be considered. It is well known that there are major fatigue fracture modes

for the high-strength metals. One is caused mainly by non-metallic inclusion, and no GBF can be clearly observed on the fracture surface. The fatigue life varies usually from 10^5 cycles to 10^7 cycles [17].

Fatigue strength is one of the component that is effected by surface roughness. However, high strength metals generally contain very high sensitivity to surface fault which is similar for porosity structure surface, such as surface cut, and machining faults, which roughen the surface. Murakami and Endo [18] tackled $\text{Area}^{1/2}$ parameter model for the prediction of the fatigue limit of samples with small defects and applied this model to the specimens with artificial surface roughness.

CONCLUSION

Scientific computing plays a major role in understanding the way nature designs and constructs its structures. Computer simulations can explore complex natural phenomena inaccessible for researchers. Meanwhile, accessibility to high performance computing and advanced computer modelling languages for researchers has increased tremendously. Along with the theory and experimentation, scientific computer modelling has become an important tool for scientific discoveries [19]. Porosity structures widely used in medical field in order to create light weight design to avoid density effect or increase bone-implant interaction.

Developing finite element method for cellular structure may help to improve producing better mechanical performance metal foams. Before developing finite element model of cellular structure, why it is important to adjust or progress of fatigue failure has to be deified. Theoretically 3D printers can produce perfect network connectors however, in reality some of the wall may missing in the structure. these features effects can be calculate with FEM approach. Some of the commercially available implants which are mentioned in introduction section. Fatigue calculation may postpone the failure station in order to adjust mesh architect and changing failure coordinates. On the other hand, it is quite vital to understand failure of porosity structure or small crack how effect the all implant systems. Therefore, small structure failure may not lead to implant failure if crack of connectors in not in load direction.

As it was mentioned during calculation mechanical performance depends on several dynamics such as properties of solid, relative density, geometry, cell shape and foams types open or closed cells. However, in this paper cell size adjusted considering interaction bone cells and porosity structure. Because only range of porosity size bone can grove in the cell. It is quite known that open cell has to be chosen in order to mimics bone behavior. Material should be biocompatible and ASTM standards explains what sort of material has to be used. Therefore, improving mechanical performance of light-weight implants, relative density and cell shape should be optimized and it proves that approach and problem solving theory in this paper is decided reason given above.

References

- [1] Ashby MF, Evans A, Fleck NA, Gibson LJ, Hutchinson JW, Wadley HNG: *Metal Foams: A Design Guide: Elsevier Science; 2000.*
- [2] Gibson, L.J., Ashby, M.F., 1997. *Cellular Solids: Structure and Properties, second ed. Cambridge University Press, Cambridge.*
- [3] ASTM Committee F42 on Additive Manufacturing Technologies.
- [4] M. Alemán, A. Streek, P. Regenfuß, A. Mette, R. Ebert, H. Exner, S.W. Glunz, G. Willeke, *Laser micro-sintering as a new metallization technique for silicon solar cells, Proceedings of the 21st European Photovoltaic Solar Energy Conference, Dresden, 2006*
- [5] Clarke DR: *Interpenetrating Phase Composites. Journal of the American Ceramic Society 1992.*
- [6] Gibson LJ. *The mechanical behavior of cancellous bone. J. Biomech. 1985; 18: 317-328.*
- [7] Arthur TL. *Thesis proposal: Fatigue damage in trabecular bone. MIT, 1998.*
- [8] Anderson TL. *Fracture Mechanics. CRC Press, 1995; 69-72.*
- [9] Levan and Royer, 1993; Murakami, 1987; Rooke and Cartwright, 1976
- [10] Levan A and Royer J. *Part-circular surface cracks in round bars under tension, bending and twisting. Intl j Fract 1993; 61: 71-99.*
- [11] Paris PC and Erdogan F. *Trans. ASME 1963; 85: 528.*
- [12] Bathias C. *There is no infinite fatigue life in metallic materials. Fatigue Fract Eng Mater Struct 1999;22:559-65.*
- [13] Nakamura, T., Kaneko, M., Noguchi, T., Esaka, T. and Jinbo, K., *Super-long fatigue properties of a steel tempered at low temperature. In Proceedings of the 23rd Fatigue Symposium, Soc. Mat. Sci. Jpn, 1996, pp. 245-248*
- [14] Murakami, Y., *Metal fatigue: effects of small defects and nonmetallic inclusions. Yokendo Ltd., Tokyo, 1993.*
- [15] Murakami, Y., *Quantitative evaluation of effects of defects and non-metallic inclusions on fatigue strength of metals. Iron Steel Inst. Jpn, 1989, 75(8), 1267-1277.*
- [16] Chapetti MD, Tagawa T, Miyata T. *Ultra-long cycle fatigue of high-strength carbon steels part I: review and analysis of the mechanism of failure. Mater Sci Eng A 2003;356:227-35.*
- [17] Murakami Y. *Metal fatigue: effects of small defects and nonmetallic inclusions. Amsterdam and Boston: Elsevier; 2002. p. 6.*
- [18] Murakami Y, Endo M. *Effects of defects, inclusions and inhomogeneities on fatigue strength. Int J Fatigue 1994;16:163-82*
- [19] Padma R, Simon HD: *Parallel processing for scientific computing. In.: SIAM; 2006*